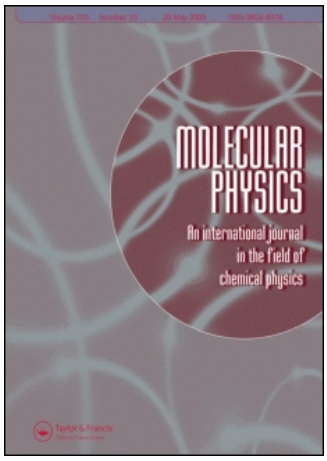

Molecular Physics
An International Journal in the Field of Chemical Physics
Publication details, including instructions for authors and subscription information:
http://www.informaworld.com/smpp/title~content=t713395160

Singlet-triplet oscillations of spin-correlated radical pairs due to the Larmor precession in low magnetic fields

V. A. Bagryansky; V. I. Borovkov; Yu. N. Molin

To cite this Article: Bagryansky, V. A., Borovkov, V. I. and Molin, Yu. N. , 'Singlet-triplet oscillations of spin-correlated radical pairs due to the Larmor precession in low magnetic fields', Molecular Physics, 100:8, 1071 - 1078
To link to this article: DOI: 10.1080/00268970110109484
URL: http://dx.doi.org/10.1080/00268970110109484

MOLECULAR PHYSICS, 2002, VOL. 100, NO. 8, 1071–1078

Singlet–triplet oscillations of spin-correlated radical pairs due to the Larmor precession in low magnetic fields

V. A. BAGRYANSKY[1,2], V. I. BOROVKOV[1,2] and YU. N. MOLIN[1]*

[1] Institute of Chemical Kinetics and Combustion, Novosibirsk 630090, Russia
[2] Novosibirsk State University, Novosibirsk 630090, Russia

(*Received 17 July 2001; accepted 4 September 2001*)

Singlet–triplet oscillations in spin-correlated radical pairs have been studied at magnetic field strengths low for one radical and high for the other. Oscillations with frequencies close to the Larmor frequency ω_0 of electron spin precession have been predicted under these conditions. Both numerical and exact analytical solutions in arbitrary magnetic fields are presented for three cases of hyperfine couplings in wide-spectrum radical. For the case of unresolved spectrum, singlet–triplet evolution was found to contain a single oscillating term with frequency ω_0. In the case of one spin-I magnetic nucleus, there are two low frequency oscillating terms with frequencies $\omega_- = \omega_0 - \omega_0/(2I+1)$ and $\omega_+ = \omega_0 + \omega_0/(2I+1)$, the amplitude of the first term being larger than that of the second. The case of a number of equivalent protons also has been analysed as a superposition of one-nucleus oscillations. The predicted oscillations were observed in a time resolved magnetic field effect for several radical ion pairs produced by X-ray irradiation of alkane solutions with charge acceptors. For pairs (*p*-terphenyl-d_{14})$^{-\bullet}$/(iso-octane)$^{+\bullet}$ and (*p*-terphenyl-d_{14})$^{-\bullet}$/(2,4-dimethylpentane)$^{+\bullet}$ the oscillation frequency in a field B_0 of 0.5–4 mT is about 20% lower than ω_0. Oscillations were observed also in pairs with equivalent nuclei: (*p*-terphenyl-d_{14})$^{+\bullet}$/$(C_6F_6)^{-\bullet}$ and (*p*-terphenyl-d_{14})$^{-\bullet}$/(hexamethylethane)$^{+\bullet}$.

1. Introduction

It is well known that magnetic fields can affect chemical reactions that involve radical pairs as intermediates [1, 2], and there has been much interest in the effects of low fields comparable with the Earth's magnetic field (~0.05 mT). The intensity of such fields is significantly lower than typical hyperfine coupling constants in radicals (1–10 mT), which suggests that the conventional magnetic effect resulting from Zeeman splitting of spin levels in a magnetic field should be ineffective. However, both experiment and theory show that, for long-lived radical pairs, weak magnetic fields can considerably affect reaction yields [3–6]. Investigations into this effect are of interest due to the possible influence of ambient electromagnetic radiation on living organisms [7] and the mystery of animal navigation [8].

One of the highly effective tools for investigating the mechanism of magnetic field effects in chemical reactions is time resolved magnetic field effect (TR MFE) in recombination fluorescence [9, 10]. In TR MFE experiments a short pulse of ionizing irradiation produces radical ion pairs in a singlet correlated spin state that can evolve under the influence of external magnetic field, hyperfine coupling (HFC) and relaxation. A luminophore with high fluorescence quantum yield is usually selected as a charge acceptor, to produce singlet excited molecules in recombination of singlet pairs. Fluorescence kinetics of the molecules thus provides information about time evolution of the population of the singlet state of the pair $\rho_{ss}(t)$. Such information is a key to understanding the origin of magnetic field effects, as long as they arise through the spin dynamics of a radical pair being affected by a magnetic field. Good time resolution and sensitivity of the technique are ensured by optical registration methods.

In TR MFE experiments the spin dynamics in a high field usually are compared with those in zero field. This technique has been used to study: (i) systems where radical cations and anions have narrow ESR spectra and different g values [11–16]; (ii) pairs with one of the radical ions having HFC with a number of equivalent nuclei [17–20]; and (iii) pairs of radical ions with ESR spectrum unresolved due to HFC with many magnetic nuclei [21, 22]. In these particular cases, spin dynamics in a high or zero magnetic field can be calculated analytically and there is a comparatively simple frequency spectrum, thus allowing for clear interpretation of experimental results.

The general case of HFC with non-equivalent magnetic nuclei requires the numerical calculation of spin

* Author for correspondence. e-mail: molin@ns.kinetics.nsc.ru

Molecular Physics ISSN 0026–8976 print/ISSN 1362–3028 online © 2002 Taylor & Francis Ltd
http://www.tandf.co.uk/journals
DOI: 10.1080/00268970110109484

dynamics. The frequency spectrum of $\rho_{ss}(t)$ is very rich in this case, thus complicating the interpretation of experiments. Similar difficulties appear in the case of a low magnetic field $B_0 \leqslant A_{HFC}$, where the oscillation frequencies of the spin population $\rho_{ss}(t)$ depend on both HFC constants and field intensity B_0.

The present paper discusses peculiarities in the spin dynamics for a magnetic field that is high with respect to one partner of the radical pair and low (or intermediate) for the other. This can be achieved when the ESR spectrum widths of the radical partners differ greatly. It is shown that under such conditions TR MFE curves exhibit oscillations with a frequency close to the Larmor frequency of electron spin precession in magnetic field B_0. The first experimental evidence of this phenomenon is provided.

2. Theory and simulation

If there is no interaction between spins S_A and S_B of the pair partners, the probability of finding the pair in the singlet state, provided it is initially singlet, is expressed in terms of product of spin correlation tensors ${}_A\mathbf{T}$ and ${}_B\mathbf{T}$ [23]

$$\rho_{ss}(t) = \tfrac{1}{4} + {}_A\mathbf{T} : {}_B\mathbf{T} = \tfrac{1}{4} + \sum_{m,n=x,y,z} ({}_AT_{mn})({}_BT_{mn}). \quad (1)$$

The components of the tensor connected with the spin projection operators in the Schrödinger representation are S_{Ai}, S_{Bi} and in the Heisenberg representation are $S_{Ai}(t)$, $S_{Bi}(t)$ $(i = x, y, z)$, and

$${}_AT_{mn} = Sp\langle S_{Am} S_{An}(t)\rangle, \quad (2)$$

where Sp stands for the trace over electron spin variables, and the pointed brackets denote averaging over projections of magnetic nuclei.

In experiments, information about spin dynamics is obtained from an analysis of TR MFE curves given by the ratio of recombination fluorescence intensity with applied magnetic field to that without magnetic field, $I_H(t)/I_0(t)$ [9, 10, 18–20]. This method of registration excludes the sharply decaying in time and poorly determined factor in the $I(t)$ dependence proportional to the recombination rate of radical pairs. Considering also that not all the pairs in radiation tracks are formed in a singlet correlated spin state, we find the ratio to be

$$\frac{I_H(t)}{I_0(t)} = \frac{\theta\rho_{ss}^H(t) + \frac{1}{4}(1-\theta)}{\theta\rho_{ss}^0(t) + \frac{1}{4}(1-\theta)}, \quad (3)$$

where θ is the fraction of singlet-correlated pairs.

Let us consider the case when radical A has a broader ESR spectrum than that of its partner B, and the external magnetic field is considerably greater than the width of the ESR spectrum of radical B. Major peculiarities of spin dynamics in this case can be most clearly illustrated under the restriction that the HFC in radical S_B is negligible. Then

$${}_BT_{xx} = {}_BT_{yy} = \tfrac{1}{2}\cos\omega_0 t, \qquad {}_BT_{yx} = -{}_BT_{yx} = \tfrac{1}{2}\sin\omega_0 t,$$
$${}_BT_{zz} = \tfrac{1}{2}, \quad (4)$$

where $\omega_0 = \gamma B_0$ (γ is the gyromagnetic ratio for electron spin). Also, let us assume all the pairs to be correlated $(\theta = 1)$, paramagnetic relaxation to be absent, and the g factors of the radicals to be equal to that of free electron. We shall measure the intensity of the magnetic field and the values of the HFC constants a in units of circular frequency $(a = \gamma A)$.

2.1. *Unresolved spectrum: quasiclassical approximation*

If radical A has an HFC with a large number of magnetic nuclei, a calculation becomes possible within the framework of quasiclassical approximation [23], where variation of the nuclear spin states with time is neglected. Then the time independent HFC term in the Hamiltonian can be treated as an internal magnetic field, the projections of which have a Gaussian distribution with the second momentum σ^2 equal to

$$\sigma^2 = \frac{1}{3}\sum_k a_k^2 I_k(I_k+1), \quad (5)$$

where I_k is spin of nucleus with HFC constant a_k.

The distribution $f(\omega, \theta, \varphi)$ over absolute values of the total field ω, which is the sum of the external and internal fields, and over the angles θ and φ, which determine direction of the field, is given by

$$f(\omega,\theta,\varphi) = \frac{1}{(\sigma\sqrt{2\pi})^3}\exp\left(\frac{-(\omega\cos\theta - \omega_0)^2 + \omega^2\sin^2\theta}{2\sigma^2}\right) \times \omega^2\sin\theta. \quad (6)$$

Reference [23] gives expressions for the coupling coefficients between operators $S_{Ai}(t)$ and operators S_{Ai} after averaging over horizontal angle φ. Having averaged the coefficients over distribution (6), using definition (2) we obtain expressions for the nonzero components of the spin correlation tensor:

$${}_AT_{xx} = {}_AT_{yy} = \tfrac{1}{2}e^{-(\sigma^2t^2/2)}\left(\cos\omega_0 t - \frac{\sigma^2 t}{\omega_0}\sin\omega_0 t\right) - \tfrac{1}{6}e^{-(\omega_0^2/2\sigma^2)}\left((1-\sigma^2t^2)e^{-(\sigma^2t^2/2)} - 1\right) + \tfrac{1}{2}I(\omega_0,\sigma,t), \quad (7)$$

$${}_AT_{zz} = \tfrac{1}{2} + \tfrac{1}{3}e^{-(\omega_0^2/2\sigma^2)}((1-\sigma^2t^2)e^{-(\sigma^2t^2/2)} - 1) - I(\omega_0,\sigma,t), \quad (8)$$

$$ {}_{\mathrm{A}}T_{yx} = -{}_{\mathrm{A}}T_{xy} = \tfrac{1}{2}\mathrm{e}^{-(\sigma^2 t^2/2)} \times \left(\left(1 - \frac{\sigma^2}{\omega_0^2} \right) \sin\omega_0 t + \frac{\sigma^2 t}{\omega_0} \cos\omega_0 t \right), \quad (9) $$

where

$$ I(\omega_0, \sigma, t) = \frac{1}{\sqrt{2\pi}} \int_0^\infty (\cos\omega t - 1)\, \mathrm{e}^{-((\omega^2+\omega_0^2)/2\sigma^2)} \times \left[\mathrm{e}^{(\omega\omega_0/\sigma^2)} \frac{\sigma}{\omega_0^2} \left(\frac{\sigma^2}{\omega\omega_0} - 1 \right) - \mathrm{e}^{-(\omega\omega_0/\sigma^2)} \frac{\sigma}{\omega_0^2} \left(\frac{\sigma^2}{\omega\omega_0} + 1 \right) + \frac{2\omega^2}{3\sigma^3} \right] \mathrm{d}\omega. \quad (10) $$

For small values of the ratio ω_0/σ integral $I(\omega_0, \sigma, t)$ vanishes. Substituting the elements of tensors (4) and (7)–(9) in equation (1) we can obtain the dependence $\rho_{\mathrm{ss}}^{\mathrm{H}}(t)$, integral (10) being calculated numerically. Substitution of $\rho_{\mathrm{ss}}^{\mathrm{H}}(t)$ along with the known expression for zero external field [23],

$$ \rho_{\mathrm{ss}}^{0}(t) = \tfrac{1}{2} + \tfrac{1}{2}(1 - \sigma^2 t^2)\, \mathrm{e}^{-(\sigma^2 t^2/2)}, \quad (11) $$

in equation (3) gives the TR MFE illustrated with examples for $\omega_0 = 2\sigma$, σ and 0.5σ in figure 1. Distinct oscillations with frequency ω_0 are observed. Their amplitude is almost independent of field intensity for $\omega_0 \leqslant \sigma$ and decreases with the ratio ω_0/σ. The appearance of such oscillations also follows directly from the expression for $\rho_{\mathrm{ss}}^{\mathrm{H}}(t)$ at $\omega_0 \ll \sigma$, which in this limiting case is given by

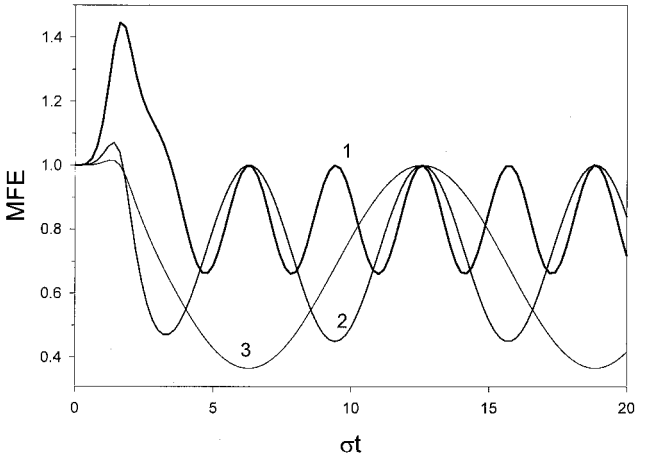

Figure 1. Calculated TR MFE in quasiclassical approximation for different ratios of the external field intensity ω_0 to the spectrum width parameter σ of one of the radicals in the pair: 1, $\omega_0/\sigma = 2$; 2, $\omega_0/\sigma = 1$; and 3, $\omega_0/\sigma = 0.5$. The other radical has no HFC.

$$ \rho_{\mathrm{ss}}^{\mathrm{H}}(t) \approx \tfrac{1}{3} + \tfrac{1}{6}\cos\omega_0 t[1 - (1 - \sigma^2 t^2)\, \mathrm{e}^{-(\sigma^2 t^2/2)}] + \tfrac{2}{3}(1 - \sigma^2 t^2)\, \mathrm{e}^{-(\sigma^2 t^2/2)}. \quad (12) $$

The origin of these oscillations is connected with the Larmor precession of spin $\mathrm{S_B}$ about the direction of the external field. The precession modulates the singlet population of the pair. Within the frame of the quasiclassical model, the rapid precession of spin $\mathrm{S_A}$ about randomly oriented internal field results in partial loss of spin correlation at times $t \geqslant \sigma^{-1}$.

2.2. *Radical with one magnetic nucleus*

Calculations of spin dynamics in an external magnetic field for the case when radical A contains only one magnetic spin-I nucleus with HFC constant a are given in [1, 24, 25]. Let us provide only final equations in the form used for calculations in this work. Nonzero components of spin correlation tensor are

$$ {}_{\mathrm{A}}T_{xx} = {}_{\mathrm{A}}T_{yy} = \tfrac{1}{2}\,\mathrm{Re}\, h_{\mathrm{A}}(t), \quad {}_{\mathrm{A}}T_{xy} = -{}_{\mathrm{A}}T_{yx} = \tfrac{1}{2}\,\mathrm{Im}\, h_{\mathrm{A}}(t), \quad {}_{\mathrm{A}}T_{zz} = \tfrac{1}{2} g_{\mathrm{A}}(t), \quad (13) $$

where

$$ g_{\mathrm{A}}(t) = 1 - \frac{a^2}{2I+1} \sum_{m=-\mathrm{I}}^{\mathrm{I}} \frac{I(I+1) - m(m+1)}{(2R_m)^2} \times [1 - \cos(2R_m t)], \quad (14) $$

$$ h_{\mathrm{A}}(t) = \frac{1}{4(2I+1)} \sum_{m=-\mathrm{I}}^{\mathrm{I}} [(1 + D_m)\, \mathrm{e}^{\mathrm{i}R_m t} + (1 - D_m)\, \mathrm{e}^{-\mathrm{i}R_m t}] \times [(1 + D_{m-1})\, \mathrm{e}^{\mathrm{i}R_{m-1} t} + (1 - D_{m-1})\, \mathrm{e}^{-\mathrm{i}R_{m-1} t}], \quad (15) $$

$$ 2R_m = [\omega_0^2 + a\omega_0(2m+1) + a^2(I + \tfrac{1}{2})]^{1/2}, \quad (16) $$

$$ D_m = \frac{\omega_0 + a(m + \frac{1}{2})}{2R_m}. \quad (17) $$

Substituting the values of tensor components (4) and (13) in equation (1) we obtain

$$ \rho_{\mathrm{ss}}^{\mathrm{H}}(t) = \tfrac{1}{4} + \tfrac{1}{4} g_{\mathrm{A}}(t) + \tfrac{1}{2}\,\mathrm{Re}(h_{\mathrm{A}}(t)\, \mathrm{e}^{-\mathrm{i}\omega_0 t}). \quad (18) $$

Similarly to the quasiclassical case, in order to reveal the low frequency oscillations we can simplify equation (18) in the limit $\omega_0 \ll a$ Then the spectrum of function $\rho_{\mathrm{ss}}^{\mathrm{H}}(t)$ will contain both high frequencies

$$ 2R_m \approx a(I + \tfrac{1}{2}) + \omega_0 \frac{2m+1}{2I+1}, \quad R_m + R_{m-1} \pm \omega_0 \approx a(I + \tfrac{1}{2}) + \omega_0 \left(\frac{2m}{2I+1} \pm 1 \right), \quad (19) $$

and low frequencies

$$\omega_{\pm} = \omega_0 \pm (R_m - R_{m-1}) \approx \omega_0 \left(1 \pm \frac{1}{2I+1}\right). \qquad (20)$$

Neglecting terms of order smaller than ω_0/a in equation (18) one obtains

$$\rho_{ss}^{H}(t) \approx \frac{1}{3} + \frac{1}{6(2I+1)^2} + \frac{(I+1)(2I+3)}{6(2I+1)^2} \times \cos\left(\left(1 - \frac{1}{2I+1}\right)\omega_0 t\right) + \frac{I(2I-1)}{6(2I+1)^2} \times \cos\left(\left(1 + \frac{1}{2I+1}\right)\omega_0 t\right) + \text{high frequency terms.} \qquad (21)$$

High frequency terms in equation (21) have frequencies (19) in the interval $a(I+\frac{1}{2}) \pm \omega_0$. Their contribution in $\rho_{ss}^{H}(t)$ decays within a time of the order of $2\pi/\omega_0$. As one can see from equation (21), the amplitude T of oscillations with frequency ω_- is greater than that for ω_+:

$$\frac{T(\omega_-)}{T(\omega_+)} = \frac{(I+1)(2I+3)}{I(2I-1)} > 1. \qquad (22)$$

Note that $T(\omega_+) = 0$ for $I = 1/2$. Comparing equation (12) with equation (21) for large values of nuclear spin $I \gg 1$ one can see that they give the same result after longer times $\omega_0 t \gg 1$, i.e. oscillations with the Larmor frequency and an amplitude of 1/6. Figure 2 shows the result of a calculation of the population $\rho_{ss}^{H}(t)$ for nuclear spin $I = 9$ (curve 1) and $I = 3$ (curve 2) at $\omega_0 = 0.5a$. For comparison, the figure also shows the result of a calculation of radical pair spin dynamics in the quasiclassical approximation at $\sigma = 2a$ (curve 4). As seen on the figure, for spin $I = 9$ the high frequency oscillations decay rapidly while the low frequency ones are close to those in the quasiclassical case. At the same time, in contrast to the quasiclassical case, some amplitude modulation of the low frequency oscillations is observed. This results from the beating of two close low frequencies ω_+ and ω_-.

Increase in nuclear spin I reduces deviation from the quasiclassical description. The reason of this coincidence is obvious since it is at large values of nuclear spin I that the quasiclassical approximation is justified. Vice versa, in cases of small values of the nuclear spin I (curve 2) the deviations from the quasiclassical description grow more considerably. First, the low frequency oscillation period becomes noticeably larger than the Larmor oscillation period. Second, repetitive bursts of the high frequency modulation come after shorter times (for $I = 9$ the first burst appears at time $at \sim 130$, and lies beyond the graph).

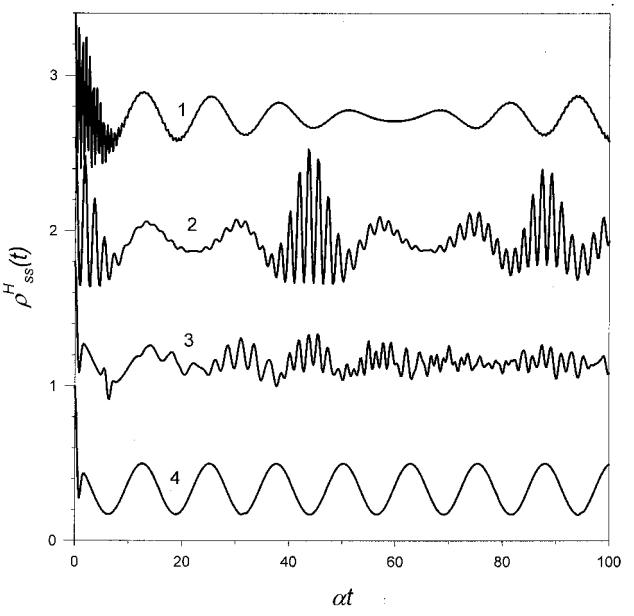

Figure 2. Calculated singlet population $\rho_{ss}^{H}(t)$ for singlet-born radical pair with HFC constant a in one of the radicals: 1, one magnetic nucleus with spin $I = 9$; 2, one magnetic nucleus with spin $I = 3$; 3, 18 magnetically equivalent nuclei with spin $I = 1/2$; and 4, uresolved ESR spectrum with the same second momentum as for curve 3 ($\sigma = 3a/\sqrt{2}$). For convenience, the curves are vertically shifted by 2.4, 1.6, and 0.8, respectively. The external field intensity is $\omega_0 = 0.5a$. The other radical has no HFC.

The presence of two low frequencies $\omega_{\pm}(20)$ in the limit $\omega_0 \ll a$ and the difference in their amplitudes can be explained using a vector model [6]. A scheme elucidating the model is shown on figure 3. In the singlet state, spins S_A and S_B are antiparallel. However, with time their relative orientation can change. The measure of the singlet population is the projection of one spin on the direction opposite to the other spin: $-(\mathbf{S}_A, \mathbf{S}_B)$. Spin S_B precesses about the direction of the external field with frequency ω_0. In a low magnetic field, spin S_A rotates rapidly about the direction of the total angular momentum, which is the vector sum of the electron and the nuclear spins $\mathbf{J}_A^{\pm} = \mathbf{I}_A \pm \mathbf{S}_A$, with a frequency determined by the HFC constant a.

For $\omega_0 \ll a$, high frequency rotation averages vector $\mathbf{S}_A$ to its projection $\mathbf{F}_A$ on vector $\mathbf{J}_A$. The sum vector $\mathbf{J}_A$ precesses about the direction of the external field. The frequency of this precession is noticeably lower than the Larmor precession frequency of an electron because in this case the magnetic momentum of the total spin is close to that of the electron spin, while its angular momentum is close to that of the nuclear spin. One can see from the figure that the rotation sign is determined by the sign in $\mathbf{J}_A^{\pm} = \mathbf{I}_A \pm \mathbf{S}_A$. Vector $\mathbf{J}_A^{+}$ precesses

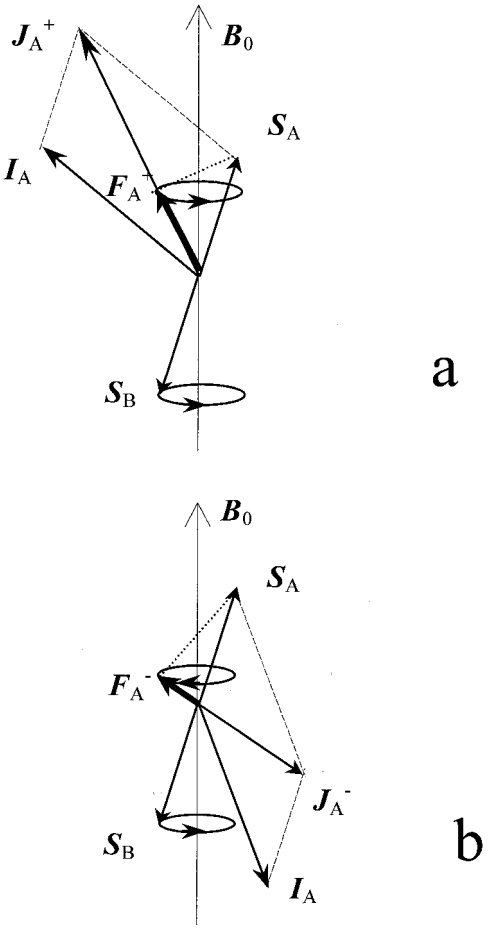

Figure 3. Schematic representation of the spin dynamics for a singlet-born radical pair by the vector model (see text).

in the same direction as the other vector $\mathbf{S}_B$, while vector $\mathbf{J}_A^-$ precesses with the opposite sign. The singlet population is modulated by the difference between the precession frequencies of the two spins, which are ω_- for $\mathbf{J}_A^+$ and ω_+ for $\mathbf{J}_A^-$.

The diagram also shows that the projection $\mathbf{F}_A^+$ of vector $\mathbf{S}_A$ on the direction $\mathbf{J}_A^+$ is larger that the projection $\mathbf{F}_A^-$ of vector $\mathbf{S}_A$ on the direction $\mathbf{J}_A^-$. That is the reason for the difference (equation (22)) between the amplitudes of the oscillations ω_- and ω_+. As the value of the nuclear spin I increases, precession of the sum spin slows down and vectors $\mathbf{J}_A^+$ and $\mathbf{J}_A^-$ align along the field and against the field, respectively, thus equalizing frequencies $\omega_\pm$ and their amplitudes.

Note that in zero magnetic field, in contrast to the field case discussed above, oscillations in $\rho_{ss}^0(t)$

$$\rho_{ss}^0(t) = \frac{1}{4} + \frac{1}{4(2I+1)^2} \times [4I(I+1) + 3 + 8I(I+1)\cos(a(I+\tfrac{1}{2})t)], \quad (23)$$

have only one high frequency $a(I+1/2)$ [1]. Therefore, the low frequency oscillations in the magnetic effect (equation (3)) are more readily observed when the high frequency terms are smoothed. In real experiments it is the limited resolution of the equipment that can lead to the smoothing with a large HFC constant.

2.3. *Radical with equivalent protons*

If radical A contains magnetically equivalent nuclei whose isotropic coupling with the electron is described by a single HFC constant equal to a, then total nuclear spin is conserved. This allows us to generalize the results obtained in the previous section by averaging the expressions therein over the distribution of the values of the total nuclear spin I. For n equivalent protons the distribution is given by

$$P_I = \frac{(2I+1)^2 n!}{2^n \left(\frac{n}{2} - I\right)! \left(\frac{n}{2} + I + 1\right)!}. \quad (24)$$

Applying this averaging to functions $g_A(t)$ and $h_A(t)$ in equation (18) one can obtain the desired result.

Curve 3 in figure 2 corresponds to calculation of $\rho_{ss}^H(t)$ for 18 equivalent nuclei at $\omega_0 = 0.5a$. One can see that $\rho_{ss}^H(t)$ includes both low frequency and high frequency oscillations. Over short times the description is close to the quasiclassical one with the same value of the second momentum, whereas over longer times they deviate considerably. The low frequency oscillation has a frequency lower than the Larmor frequency ω_0.

The deviation is caused by the large contribution of nuclear configurations with small I values. Indeed, the averaged value $\langle I \rangle = \sum_I P_I I$ of the total spin increases with the number of protons n according to approximate equation $\langle I \rangle \approx 0.75\sqrt{n}$. Thus, for $n = 18$, $\langle I \rangle \approx 3$. For the spin value $I = 3$ the difference between $\omega_\pm$ and ω_0 is about 15%, the amplitude of the lower frequency harmonics ω_- being approximately three times that of the ω_+ harmonics.

Apparently, the rise in the high frequency oscillations is also connected with the prevalence of nuclear configurations with moderate I values. Theoretically, the deviations from the quasiclassical approximation vanish at $n \gg 1$. However, since $\langle I \rangle$ grows slowly with n, a satisfactory agreement is achieved only for an unrealistically large number of equivalent protons. The problem of approaching the quasiclassical description for a finite number of non-equivalent nuclei requires further investigation.

When processing experimental results, one should take into account longitudinal T_1 and transversal T_2 paramagnetic relaxation of the radicals, and also recall that the partner radical B has a finite second momentum

σ_B^2. With these factors taken into consideration, the expression for the singlet population is given by [20]

$$\rho_{ss}^{H}(t) = \tfrac{1}{4} + \tfrac{1}{4}\,e^{-(t/T_1)}\langle g_A(t)\rangle + \tfrac{1}{2}\,e^{-(t/T_2)}\,e^{-(\sigma_B^2 t^2/2)}\,\mathrm{Re}(\langle h_A(t)\rangle\,e^{-i\omega_0 t}). \quad (25)$$

The expression for the singlet population in zero magnetic field [20], which will be used for fitting experimentally measured TR MFE in the next section, is

$$\rho_{ss}^{0}(t) = \tfrac{1}{4} + \tfrac{1}{12}e^{-(t/T_0)}[1 + 2(1-\sigma_B^2 t^2)\,e^{-(\sigma_B^2 t^2/2)}] \times \left[\frac{n+3}{n+1} + \frac{2n(n+2)}{n+1}\left(\cos\frac{at}{2}\right)^{n+1} - 2n\left(\cos\frac{at}{2}\right)^{n-1}\right]. \quad (26)$$

Here T_0 describes phase relaxation in zero field. The frequency spectrum of the singlet population (26) contains only high frequencies $a(m+\frac{1}{2})$, $m = 0, 1, \ldots, n/2$. This means that when harmonics with frequencies higher than a are smoothed, the TR MFE curve (3) will display only low frequency oscillations. As an illustration, figure 4 shows the calculation for 18 equivalent protons in comparison with the quasiclassical calculation. Instrument smoothing was simulated by averaging over a rectangular time slot with width $\Delta = 4\pi/a$.

3. Experimental

The luminescence of *n*-hexane solutions was detected by the single-photon counting technique using an X-ray fluorimeter described elsewhere [26]. The duration of the ionizing pulse was < 2 ns. The light was collected using an optical bandpass filter (260–390 nm). The sample cuvette was similar to that described elsewhere [27]. It was constructed to avoid the irradiation of quartz parts of the cuvette and to minimize the background luminescence.

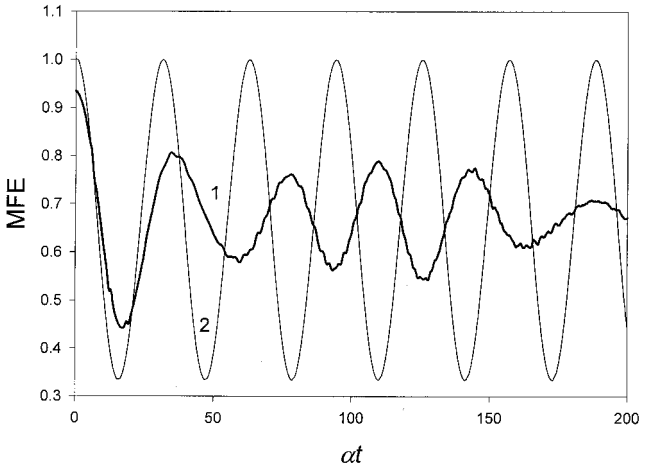

Figure 4. Calculated TR MFE (curve 1) for the case of 18 magnetically equivalent protons with HFC constant a in one of the partners and no HFC in the other one. The singlet populations $\rho_{ss}^{H}(t)$ and $\rho_{ss}^{0}(t)$ are averaged over a rectangular time slot with a width $\Delta = 4\pi/a$. The external field intensity is $\omega_0 = 0.2a$. Curve 2 is a similar calculation for an unresolved spectrum with the same second momentum.

To decrease the influence of instrumental drift the fluorescence decays were registered for periods of 250 s, alternatively with and without the magnetic field using computer control. The magnetic field was adjusted to within ± 0.05 mT.

Hexane was stirred with concentrated sulphuric acid, washed with water, distilled over sodium and passed through a 1 m column of activated alumina, coated with $AgNO_3$. The concentration of unsaturated hydrocarbon impurities was < 10 ppm. *p*-terphenyl-d_{14} (PTP-d_{14}, 98%), hexamethylethane (99%), 2,4-dimethylpentane (99%), *iso*-octane (99%), and hexafluorobenzene (99%) were used as received from Aldrich. The solutions were degassed by repeated freeze–pump–thaw cycles. All measurements were made at 293 ± 0.5 K.

4. Experimental results and discussion

As systems that could be close to the quasiclassical case we studied radical pairs $(RH)^{\bullet+}/(PTP\text{-}d_{14})^{\bullet-}$, where RH was a branched alkane molecule. From experiments in cryogenic matrices it is known that the full span of the EPR spectrum of a branched alkane can exceed 10–20 mT, the largest proton HFC constants being of about 4 mT [28]. At room temperatures one can expect the HFC constants to decrease and the number of interacting protons to increase, due to conformation transitions and the rotation of methyl groups, while the full span of the ESR spectrum remains large. Because the spectrum width of $(PTP\text{-}d_{14})^{\bullet-}$ is small ($\sigma_{PTP} = 0.068$ mT), external magnetic fields satisfying the condition $\sigma_{PTP} \ll \omega_0 < \sigma_{RH}$ can be readily met for such pairs.

Among the systems studied, the most distinct oscillations were observed for the $(iso\text{-octane})^{\bullet+}/(PTP\text{-}d_{14})^{\bullet-}$ radical pair. The HFC constants in the *iso*-octane radical cation are unknown. However, experiments on quantum beats arising under microwave pumping [29] suggest that the $(iso\text{-octane})^{\bullet+}$ radical cation has a sufficiently wide ESR spectrum. The high field TR MFE curve of this radical cation has no characteristic sharp peaks, thus indicating that not all of its protons are equivalent.

Figure 5 shows TR MFE for a solution of 0.3 M *iso*-octane + 3×10^{-5} M PTP-d_{14} in *n*-hexane in the magnetic field intensity range 0.5–4 mT. The frequency of the oscillations observed increases with magnetic field intensity and equals approximately $0.8\omega_0$. For compar-

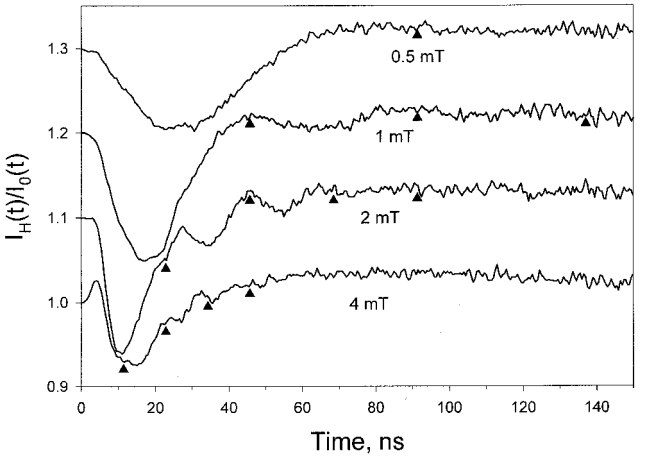

Figure 5. Experimental TR MFE for a solution of 0.3 M *iso*-octane $+3 \times 10^{-5}$ M PTP-d_{14} in *n*-hexane in magnetic fields of 0.5, 1, 2, and 4 mT. For convenience, the curves are vertically shifted by 0.3, 0.2, and 0.1, respectively. The triangles indicate predicted positions of the maxima of $0.8\omega_0$ frequency oscillations.

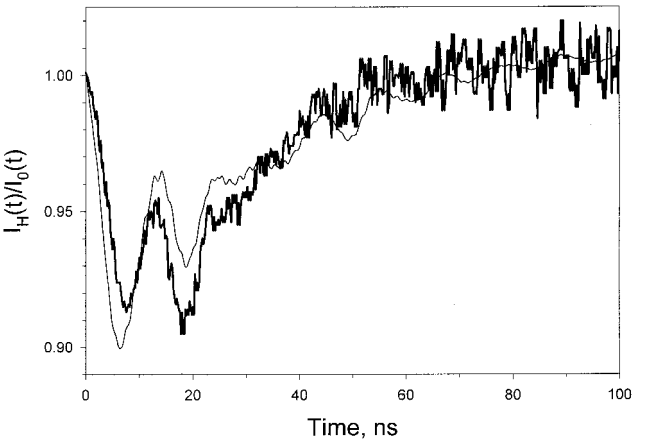

Figure 6. Experimental TR MFE for a solution of 10^{-2} M hexafluorobenzene $+10^{-3}$ M PTP-d_{14} in *n*-hexane in a magnetic field of 4 mT. The thin line shows a simulation of the experiment by a model with 6 equivalent magnetic nuclei $I=1/2$ with the following parameter values: $a = 13.5$ mT, $T_0 = 59$ ns, $T_1 = 134$ ns, $T_2 = 59$ ns, $\theta = 0.1$, $\tau_{fl} = 1.2$ ns, and $\Delta = 2$ ns.

ison, estimated times of expected maxima of $0.8\omega_0$ frequency oscillations are shown for each field with triangles. The frequency is lower than the Larmor frequency, apparently because the number of protons in the radical seems to be insufficient to justify the quasiclassical description as discussed above. The experiment also differs from the quasiclassical case in exhibiting a deep minimum after short times and some deviation of the field dependence of the oscillation frequency from linear when the field intensity is increased from 2 mT to 4 mT. Similar oscillations were obtained also for the pair (2,4-dimethylpentane)$^{\bullet+}$/(PTP-d_{14})$^{\bullet-}$ in *n*-hexane.

As an example of a radical ion with equivalent nuclei $I = 1/2$ and a large HFC constant we chose the (hexafluorobenzene)$^{\bullet-}$ radical anion with (PTP-d_{14})$^{\bullet+}$ as partner radical. The HFC constant for the fluorine nuclei is 13.5 mT [30], which corresponds to a high frequency oscillation period of the order of $2\pi/a = 2.6$ ns. As one can see from figure 6, the high frequencies do not appear clearly in the TR MFE curve measured for a field of 4 mT because their period is comparable with the fluorescence time of PTP-d_{14} ($\tau_{fl} = 1.2$ ns [13]) and the resolution of the equipment $\tau_{res} \approx 2$ ns as well.

This fact facilitates the occurrence of decaying low frequency oscillations, the position and intensity of which were fitted satisfactorily using relation (3), where the convolution product of spin populations (25) and (26) with exponential fluorescence kinetics and a rectangular instrument function were substituted. The fitting variables were relaxation times T_0, T_1, T_2 and the fraction of singlet-correlated pairs θ. The best values of these parameters are given in the legend to figure 6.

Another example of a radical with equivalent nuclei is (hexamethylethane)$^{\bullet+}$, which has 18 equivalent protons with an HFC constant of 1.22 mT [31]. An experiment in a field of 2 mT (figure 7) demonstrates a complex oscillation pattern. In this case the external field is comparable with the HFC constant. Therefore, the oscillations produced by the Larmor precession cannot be revealed. Nevertheless, the pattern as a whole is perfectly simu-

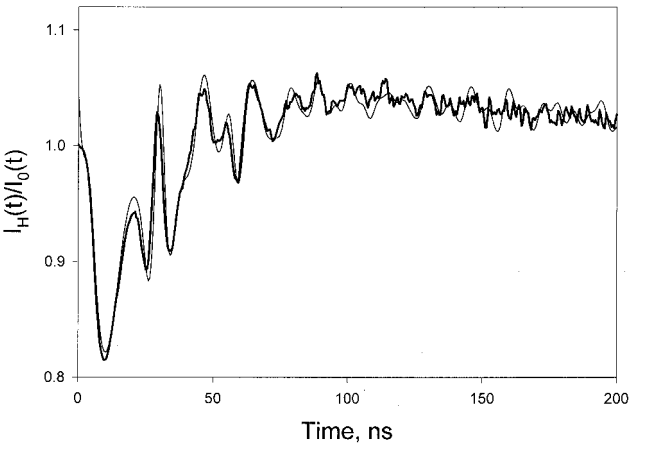

Figure 7. Experimental TR MFE for a solution of 0.3 M hexamethylethane $+3 \times 10^{-5}$ M PTP-d_{14} in *n*-hexane in magnetic fields of 2 mT. The thin line shows a simulation of the experiment by a model with 18 equivalent protons with the following parameter values: $a = 1.22$ mT, $T_0 = 40$ ns, $T_1 = 400$ ns, $T_2 = 71$ ns, $\theta = 0.22$, $t_{fl} = 1.2$ ns, and $\Delta = 2$ ns.

lated by the theory (equations (25) and (26)). As in the previous example, the fitting variables were relaxation times and the fraction of singlet-correlated pairs.

5. Conclusion

TR MFE in a magnetic field higher than the ESR spectrum width in one of the radicals of a spin-correlated pair but comparable with that width in the other radical was studied. Oscillations with frequencies close to that of electron spin precession in an external magnetic field were predicted. Their accurate coincidence with ω_0 is achieved in the limit case of a large number of magnetic nuclei. For a finite number of magnetic nuclei the frequency observed is lower than ω_0.

Experiments on radicals with equivalent nuclei support the predicted patterns. Also the results of the study of radicals with non-equivalent nuclei qualitatively agree with the theoretical predictions. At the same time, some peculiarities appear in these experiments that cannot be described by a simplified model.

This work was supported by INTAS (Grant No. 99-01766) and the Russian Foundation for Basic Research (Grant No. 99-03-33158).

References

[1] Salikhov, K. M., Molin, Yu. N., Sagdeev, R. Z., and Buchachenko, A. L., 1984, *Spin Polarization and Magnetic Effects in Chemical Reactions* (Amsterdam: Elsevier).
[2] Steiner, U. E., and Ulrich, T., 1989, *Chem. Rev.*, **89,** 51.
[3] Stass, D. V., Lukzen, N. N., Tadjikov, B. M., and Molin, Yu. N., 1995, *Chem. Phys. Lett.*, **233,** 444.
[4] Stass, D. V., Tadjikov, B. M., and Molin, Yu. N., 1995, *Chem. Phys. Lett.*, **235,** 511.
[5] Timmel, C. R., Till, U., Brocklehurst, B., McLauchlan, K., and Hore, P. J., 1998, *Molec. Phys.*, **95,** 71.
[6] Till, U., Timmel, C. R., Brocklehurst, B., and Hore, P. J., 1998, *Chem. Phys. Lett.*, **298,** 7.
[7] Brocklehurst, B., and McLauchlan, K., 1996, *Intl J. Radiation Biol.*, **69,** 3.
[8] Shulten, K., and Windermuth, A., 1986, *Biophysical Effects in Steady Magnetic Fields*, edited by G. Maret, J. Kiepenheuer, and N. Boccara (Berlin: Springer-Verlag) p. 99.
[9] Brocklehurst, B., 1997, *Radiat. Phys. Chem.*, **50,** 213.
[10] Molin, Yu. N., 1999, *Bull. Korean chem. Soc.*, **20,** 7.
[11] Veselov, A. V., Melekhov, V. I., Anisimov, O. A., and Molin, Yu. N., 1987, *Chem. Phys. Lett.*, **136,** 263.
[12] Veselov, A. V., Bizyaev, V. L., Melekhov, V. I., Anisimov, O. A., and Molin, Yu. N., 1989, *Radiat. Phys. Chem.*, **34,** 567.
[13] Grigoryantz, V. M., Tadjikov, B. M., Usov, O. M., and Molin, Yu. N., 1995, *Chem. Phys. Lett.*, **246,** 392.
[14] Bagryansky, V. A., Usov, O. M., Lukzen, N. N., and Molin, Yu. N., 1997, *Appl. magn. Reson.*, **12,** 505.
[15] Usov, O. M., Grigoryantz, V. M., Tadjikov, B. M., and Molin, Yu. N., 1997, *Radiat. Phys. Chem.*, **49,** 237.
[16] Anishchik, S. V., Usov, O. M., Anisimov, O. A., and Molin, Yu. N., 1998, *Radiat. Phys. Chem.*, **51,** 31.
[17] Anisimov, O. A., Bizyaev, V. L., Lukzen, N. N., Grigoryantz, V. M., and Molin, Yu. N., 1983, *Chem. Phys. Lett.*, **101,** 131.
[18] Bagryansky, V. A., Borovkov, V. I., Molin, Yu. N., Egorov, M. P., and Nefedov, O. M., 1997, *Mendeleev Commun.*, **4,** 132.
[19] Bagryansky, V. A., Borovkov, V. I., Molin, Yu. N., Egorov, M. P., and Nefedov, O. M., 1998, *Chem. Phys. Lett.*, **295,** 230.
[20] Bagryansky, V. A., Usov, O. M., Borovkov, V. I., Kobzeva, T. V., and Molin, Yu. N., 2000, *Chem. Phys.*, **255,** 237.
[21] Borovkov, V. I., Bagryansky, V. A., and Molin, Yu. N., 2001, *Dokl. Akad. Nauk*, **377,** 505.
[22] Borovkov, V. I., Bagryansky, V. A., Yeletskikh, I. V., and Molin, Yu. N., 2001, *Molec. Phys.*, in press.
[23] Schulten, K., and Wolynes, P. G., 1978, *J. chem. Phys.*, **68,** 3292.
[24] Brocklehurst, B., 1997, *J. chem. Soc. Faraday Trans.*, **93,** 1079.
[25] Stass, D. V., Lukzen, N. N., Tadjikov, B. M., Grigoryantz, V. M., and Molin, Yu. N., 1995, *Chem. Phys. Lett.*, **243,** 533.
[26] Anishchik, S. V., Grigoryantz, V. M., Shebolaev, I. V., Chernousov, Yu. D., Anisimov, O. A., and Molin, Yu. N., 1989, *Prib. tech. eksper.*, No. 4, 74.
[27] Borovkov, V. I., Anishchik, S. V., and Anisimov, O. A., 1997, *Chem. Phys. Lett.*, **270,** 327.
[28] Nunome, K., Toriyama K., and Iwasaki, M., 1983, *J. chem. Phys.*, **79,** 2499.
[29] Anishchik, S. V., Borovkov, V. I., Ivannikov, V. I., Shebolaev, I. V., Chernousov, Yu. D., Lukzen, N. N., Anisimov, O. A., and Molin, Yu. N., 1999, *Chem. Phys.*, **242,** 319.
[30] Anisimov, O. A., Grigoryantz, V. M., and Molin, Yu. N., 1980, *Chem. Phys. Lett.*, **74,** 15.
[31] Werst, D. W., Bakker, M. G., and Trifunac, A. D., 1990, *J. Amer. chem. Soc.*, **112,** 40.